

# Optimization of the Spark Plasma Sintering Conditions for the Consolidation of Hydroxyapatite Powders and Characterization of the Obtained Products

Alessio Cuccu, Selena Montinaro, Luca Desogus, Roberto Orrù\*, Giacomo Cao

Dipartimento di Ingegneria Meccanica, Chimica e dei Materiali, Unità di Ricerca del Consorzio Interuniversitario Nazionale per la Scienza e Tecnologia dei Materiali (INSTM) - Università degli Studi di Cagliari, Piazza D'Armi, 09123 Cagliari, Italy  
 roberto.orrù@dimcm.unica.it

A comparative investigation regarding the consolidation behavior displayed by three commercially available hydroxyapatite powders during Spark Plasma Sintering (SPS) is performed in this work. Starting powders are different in terms of purity, particle size, morphology and thermochemical stability. A completely dense product without secondary species is produced by SPS at 900 °C, when starting from highly pure powders with relatively small sized particles and grains. The resulting consolidated material, consisting of sub-micrometer sized hydroxyapatite grains, exhibits optical transparency and good mechanical properties.

On the other hand, temperature levels up to 1,200 °C are needed to sinter powders with larger particles. This holds also true when relatively finer powders are used, also containing CaHPO<sub>4</sub>, are used. In both the latter cases products with coarser microstructures and/or significant amount of β-TCP, as a result of hydroxyapatite decomposition, are obtained. Optical, chemical resistance and mechanical properties of the resulting dense materials are correspondingly deteriorated.

## 1. Introduction

The use of biomaterials to repair or replace parts of human bodies has markedly increased in the last decades (Hench and Jones, 2005). In this context, a prominent role is played by calcium orthophosphates based materials, in particular hydroxyapatite (Ca<sub>10</sub>(PO<sub>4</sub>)<sub>6</sub>(OH)<sub>2</sub>), also referred to as HAp or HA, the main inorganic component of hard human tissues (bones and teeth) (Dorozhkin, 2010). Consequently, HAp has been the subject of several investigation addressed to obtain it in either bulk form or as coating (Champion, 2013). In particular, a large number of research studies have been already conducted for the fabrication of bulk HAp products using pressureless and pressure-assisted sintering methods, mainly conventional Hot Pressing (HP) or innovative Spark Plasma Sintering (SPS) techniques (Champion, 2013).

One of the main drawbacks associated to thermal processing of HAp is related to its thermochemical instability (Cihlar, 1999). Indeed, when relatively high temperature conditions are encountered during powder consolidation, HAp decomposes to produce Tri-Calcium Phosphate (Ca<sub>3</sub>(PO<sub>4</sub>)<sub>2</sub>), also indicated as TCP, or other undesired phases. Correspondingly, mechanical and biological characteristics of the resulting materials are often negatively modified.

Under such circumstances, the SPS technology offers a suitable route for the fabrication of dense ceramic products using relatively milder sintering conditions (Nikzad et al., 2013). Such advantage is related to the fact that the electric pulsed current flowing directly through the die containing the non-conductive HAp powders permits sample heating at higher rates and in shorter processing times with respect to conventional HP, where external elements are employed as heating source. Along these lines, several attempts have been recently conducted in the literature for the consolidation of HAp powders by SPS (Orrù et al., 2009). It should be noted that the sintering temperature reported in these studies to obtain nearly full dense materials vary in a rather wide interval, i.e. from 700 to 1200 °C. This feature can be ascribed to several factors. For instance, it is clear that the characteristics of the initial powders affect their sintering behaviour as well as the composition of final

products and, consequently, the related mechanical and biological properties. In addition, the use of different SPS apparatuses and sample configurations is also expected to play a certain role in this regard. Consequently, due to the different experimental conditions adopted in the various studies, it is hard to compare the corresponding results.

To provide a contribution along this direction, the effect of the characteristics of three different commercially available HAp powders on the optimal sintering temperature, as well as the composition, microstructure and mechanical properties of the resulting SPS products is systematically investigated in the present work. It should be noted that, with the only exception for the different starting powders and the sintering temperature, all the other parameters (e.g. SPS apparatus, mechanical load, heating rate, holding time, sample shape and size) are maintained unchanged in the present study.

## 2. Experimental

Three different hydroxyapatite-based powders, heretofore indicated as HAp\_a (Sigma-Aldrich, 7.1  $\mu\text{m}$  average particle size,  $\geq 90\%$  purity), HAp\_b (Alfa-Aesar, 6.3  $\mu\text{m}$  average particle size), and HAp\_c (Plasma Biototal Ltd, 32.7  $\mu\text{m}$  average particle size, Whitlockite  $< 1\%$ ), are used as starting materials in the present work. The latter ones were examined by XRD using a Philips PW 1830 X-rays diffractometer equipped with a Ni filtered Cu K $\alpha$  radiation ( $\lambda=1.5405 \text{ \AA}$ ). The powders' morphology was investigated by scanning electron microscopy (SEM, mod. S4000, Hitachi, Japan).

The HAp powders were consolidated in the form of cylindrical disks (about 15 mm diameter, 3 mm thickness) by Spark Plasma Sintering (SPS 515S model, Sumitomo Coal Mining Co Ltd) under vacuum conditions (20 Pa). This apparatus is based on the combination of a uniaxial press (50 kN) with a DC pulsed current generator (10 V, 1500 A, 300 Hz), thus simultaneously providing a pulsed electric current through the sample (when electrically conductive) and the graphite mould, along with a mechanical pressure through the punches. Details of the SPS apparatus and procedure are reported elsewhere for the sake of brevity (Musa et al., 2013).

The effect of the dwell temperature,  $T_D$ , on the product characteristics was investigated by performing all SPS experiments at constant values of the holding time ( $t_D = 5 \text{ min}$ ), the mechanical pressure ( $P = 30 \text{ MPa}$ ), and the heating rate (75  $^\circ\text{C}/\text{min}$ ), to achieve the desired value from the room temperature.

Relative densities were determined by the Archimedes' method after accurately polishing SPSed products and considering 3.16  $\text{g}/\text{cm}^3$  as theoretical value.

The microstructure of the optimal SPSed products was examined by SEM after chemical etching the polished specimens for 10 s using a 3 vol.%  $\text{HNO}_3$  solution.

The selected samples were also investigated from a mechanical point of view. A depth-sensing indentation technique was used to determine the local elastic modulus and Vickers micro-hardness.

For statistical purposes, 30 indentations were performed for each sample and for each loading condition (0.5 and 2 N). For each indentation, the load-penetration depth curve was automatically acquired and then analyzed according to the Oliver and Pharr method to evaluate the local elastic properties (Oliver and Pharr, 1992).

## 3. Results and discussion

The comparison of the XRD patterns of the starting powders is shown in Figures 1(a)-1(f) along with the corresponding SEM micrographs. On the basis of the XRD analysis it is possible to state that HAp is the only phase present in HAp\_b and HAp\_c, while a non-negligible amount of  $\text{CaHPO}_4$  was detected in HAp\_a powders. In addition, the HAp\_a and HAp\_b systems displayed relatively broad diffraction peaks, to indicate their finer microstructure, in contrast to the narrow peaks observed when considering the HAp\_c material. The granulometry of the three different types of powders (not shown here) indicated that HAp\_a and HAp\_b systems display similar fine particles, whereas HAp\_c powders are relatively coarser. This feature is clearly confirmed when examining SEM results reported in Figure 1. Specifically, both HAp\_a and HAp\_b materials generally consist of micrometer-sized aggregates made of sub-micrometer grains. In contrast, the HAp\_c product exhibits coarser particles, up to 100  $\mu\text{m}$  sized, characterized by a sponge like structure with pores down to 100 nm (Figure 1(f)).

The sample shrinkage ( $\delta$ ) and temperature profiles obtained during the consolidation process by SPS of HAp powders are reported in Figure 2(a) for the case of the HAp\_c system. Specifically, these data refer to the conditions of  $T_D = 1,200 \text{ }^\circ\text{C}$ , 75  $^\circ\text{C}/\text{min}$  heating rate,  $t_D = 5 \text{ min}$ , and  $P = 30 \text{ MPa}$ . Only minor changes in the sample shrinkage are observed during the first 10 min of the SPS process, i.e. for temperatures below 800  $^\circ\text{C}$ . On the other hand, as the temperature is raised above that level, the slope of the sintering curve rapidly increases approximately at a constant rate to reach a sample shrinkage of about 2.5 mm when the dwell

temperature is achieved. Afterwards, the  $\delta$  parameter modestly varies up to the end of the SPS experiment. A similar behavior was observed when examining the sintering curves of HAp\_a and HAp\_b systems and/or consolidation conditions investigated.

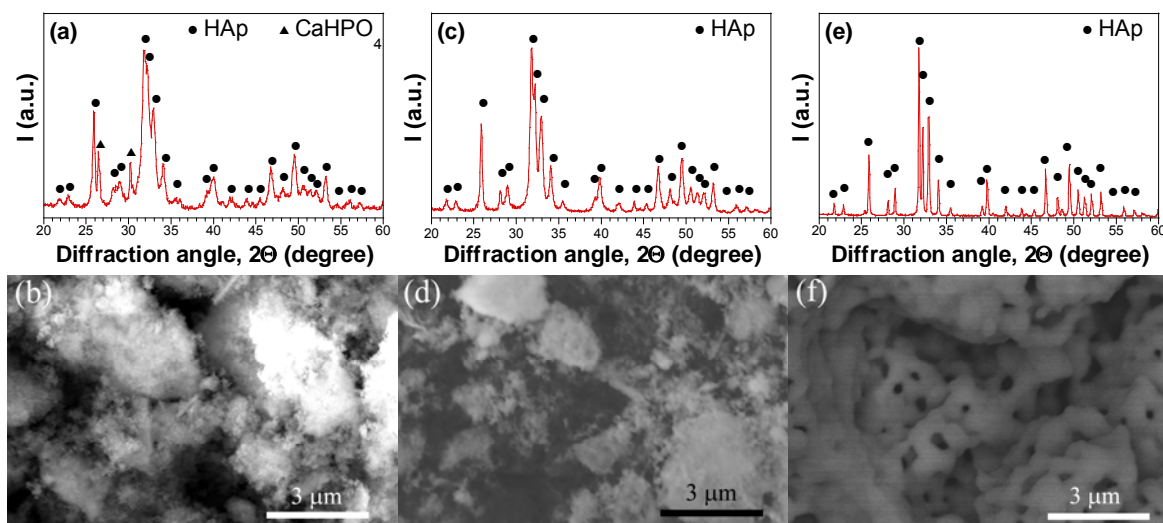


Figure 1: XRD and SEM images of the initial HAp powders used in the present work: (a)-(b) HAp\_a, (c)-(d) HAp\_b and (e)-(f) HAp\_c

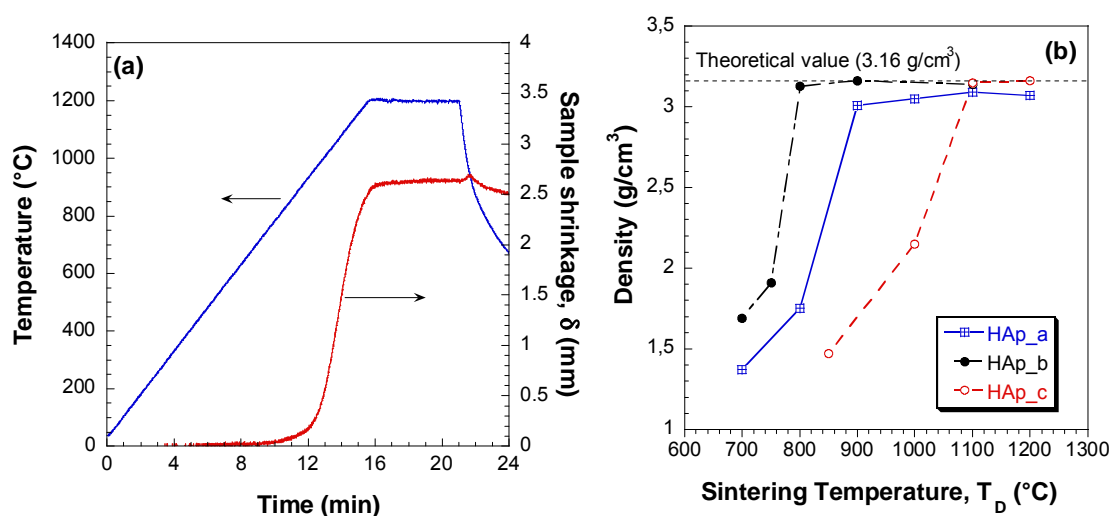


Figure 2: (a) SPS outputs profiles recorded during consolidation of HAp\_c powders and (b) dependence of final density of HAp\_a, HAp\_b, and HAp\_c sintered products on the holding temperature.

The influence of the SPS temperature on end-products density is shown in Figure 2(b) for the different HAp materials taken into account in the present work. All the plotted data refer to sintering experiments conducted at 30 MPa,  $t_D = 5$  min and 75 °C/min heating rate. As expected, the sample densification is improved as the sintering temperature is increased, although the three processed powders displayed a quite different behavior. Indeed, while the HAp\_b material achieved a high consolidation level at 800 °C, the density values obtained by the other two materials, when processed under the same conditions, are still extremely low. In particular, the temperature condition required to produce fully dense HAp\_b samples is 900 °C, whereas the optimal temperature to achieve the same goal when starting from HAp\_c powders is 1200 °C. A peculiar behavior is observed when optimizing the sintering process for the HAp\_a system. Specifically, a significant sample densification was evidenced in the range of 800 - 900 °C, while a further temperature increase was accompanied only by a slight change in product density and the theoretical density value of 3.16 g/cm<sup>3</sup> was not achieved even at 1200 °C.

The XRD patterns of the SPS products obtained for the three systems under the optimal sintering conditions is shown in Figures 3(a) - 3(f) along with the corresponding SEM micrographs.

As far as XRD analysis results are concerned, it is found that a marked decomposition of HAp to  $\beta$ -TCP, which becomes the main phase in the SPS product, is observed when processing by SPS the HAp\_a system. Minor amounts of  $\text{CaHPO}_4$  are still detected, as in the related starting powders (Figure 1(a)), while the HAp phase almost disappeared. Thus, the fact that the density of the SPSed product for the HAp\_a system does not reach the theoretical value of pure HAp (Figure 2) can be readily ascribed to the compositional changes of the processing sample during the consolidation stage.

In contrast to the behavior displayed by HAp\_a, the other two systems exhibit a higher thermochemical stability during SPS. Indeed, regardless the different dwell temperatures required to obtain fully dense materials, Figures 3(c) and 3(e) clearly indicate that no secondary phases are present in the fully dense HAp\_b and HAp\_c samples, respectively, on the basis of the XRD analysis.

Let us now examine the three SEM micrographs of the sintered products obtained by SPS under optimal conditions, after being etched with a  $\text{HNO}_3$  solution. First of all, it is seen that the HAp\_a system, mostly consisting of 1-3  $\mu\text{m}$  sized grains of  $\beta$ -TCP (Figure 3(b)), appears to be more sensitive, as compared to the other competitive materials, to the chemical etching treatment. This feature provides an indication of the fact that HAp decomposition leads products which are relatively less resistant to aggressive environments. In addition, it is clear that a relatively finer microstructure, with respect to the other systems, is obtained using HAp\_b powders, as demonstrated by the corresponding sub-micrometer sized hydroxyapatite grains evidenced by the SEM micrograph shown in Figure 3(b). In contrast, the sintered HAp\_c specimen is made of relatively coarser HA grains, up to 1-3  $\mu\text{m}$  in size. Such differences in the microstructure of the bulk products can be readily ascribed to the characteristics of the original powders as well as to the relatively milder sintering conditions required when processing HAp\_b powders (Figure 2(b)).

Three optical photos corresponding to optimal dense samples of the investigated HAp systems are also reported in the insets of Figures 3(b), 3(d) and 3(f). The product which displays a relatively higher transmission properties is HAp\_b followed by HAp\_c, whereas HAp\_a appears to be the most opaque material. Such finding is consistent with the results described above. Indeed, the HAp\_b system is obtained from the relatively more refined starting powders and no HAp decomposition was detected during the consolidation process. On the other hand, the lack of transparency in the SPSed sample obtained using HAp\_a powders could be likely associated to the significant compositional changes taking place during SPS (Figure 3(a)). Finally, although no secondary phases have been detected in the sintered HAp\_c specimen, its relatively coarse microstructure could be responsible for the corresponding lower transparency.

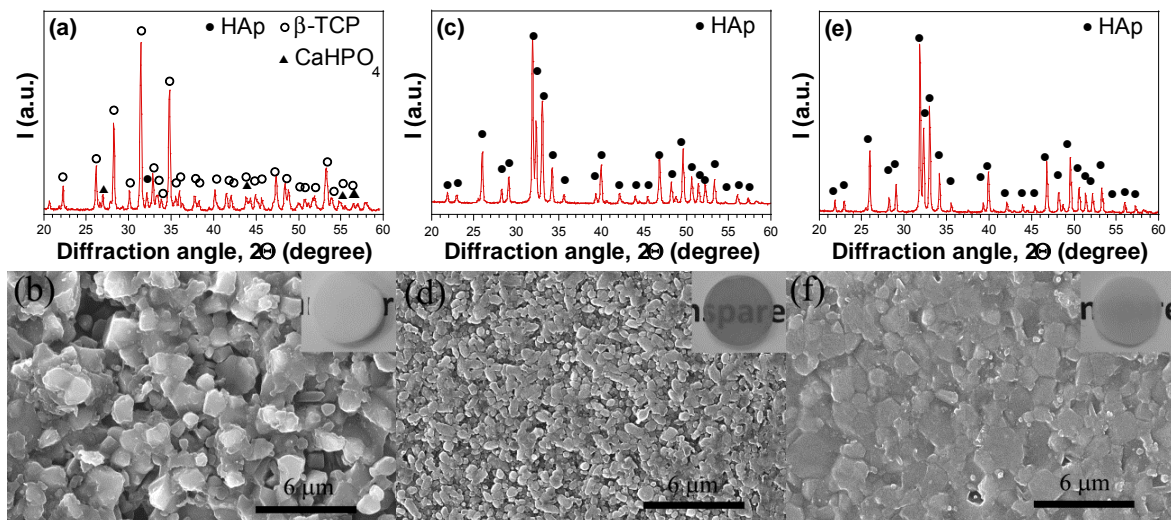


Figure 3: XRD and SEM images of optimal dense HAp products: (a)-(b) HAp\_a, (c)-(d) HAp\_b and (e)-(f) HAp\_c. Optical photographs of end-products (about 2.4 mm thick) are also shown (see insets)

The mechanical properties obtained from the indentation test performed using 0.5 N and 2.0 N loads are summarized in Table 1. It is seen that the micro-hardness of the HAp sintered bodies slightly decreases when the applied load rises from 0.5 to 2.0 N, as a result of the well-known Indentation Size Effect (ISE) (Milman et al., 2011). On the other hand, the local elastic modulus is less sensitive to the applied load, especially for HAp\_a and HAp\_b samples. Regardless of the applied load, the best local mechanical properties are achieved with the HAp\_b sintered sample. This feature can be readily associated to its composition and finer

microstructure, as described previously. Nevertheless, the relatively worse mechanical properties observed for the HAp\_a product with respect to the other two SPSed materials are probably due to HAp decomposition occurred during sintering and the corresponding incomplete densification. However, it is worth noting that, also for the HAp\_a system, the hardness value is well comparable to those ones usually reported in the literature for apatites produced with different routes. For example, hardness values in the 50-700 HV range are reported by Ramesh et al. (2013), who analyze the sintering properties of hydroxyapatite powders obtained with different methods. Moreover, values in the 200 - 500 HV range were obtained by Curran et al. (2011) when comparing undoped and Sr-doped sintered HAp samples treated at 1,200 °C. Also the local elastic modulus matches the values commonly observed for crystalline apatite solids. In particular, the results obtained in the present work are generally higher with respect to the value reported for apatites in the classical study of Gilmore and Katz (1982), i.e. 114 GPa.

*Table 1: Mechanical properties (average values) of HAp\_a, HAp\_b and HAp\_c products obtained by SPS under optimal sintering conditions: (a) micro-hardness and (b) local elastic modulus*

	Hardness (HV)		E (GPa)	
	0.5 N	2 N	0.5 N	2 N
HAp_a	530	450	120	120
HAp_b	800	750	160	165
HAp_c	760	600	150	130

#### 4. Conclusions

The comparison of the densification behaviour of three commercially available HAp-based powders and the characteristics of the obtained dense products was performed in this work taking advantage of the Spark Plasma Sintering technology. The initial powders differ in term of purity, particle size, microstructure, and thermo-chemical stability. When using the relatively small sized, with refined grains and high pure HAp\_b powders, a completely dense material without secondary phases was obtained by SPS at 900 °C. In contrast, if the coarser, albeit pure, HAp\_c powders were processed, significantly higher sintering temperatures (1,200 °C) are needed to achieve the full densification. Nevertheless, such temperature conditions are not so drastic to induce the formation of undesired phases in this material during the SPS process.

The situation changed completely when processing by SPS the HAp\_a system, whose initial fine powders also contained CaHPO<sub>4</sub>. Indeed, a significant decomposition of HAp to  $\beta$ -TCP, which becomes the major phase in the end product, was obtained at the optimal temperature (1,200 °C).

The optical, microstructural, and mechanical properties of the obtained dense bodies are consistent with the characteristics of the starting material and the corresponding SPS conditions adopted. The system exhibiting relatively higher transparency is HAp\_b, whereas the other specimens, particularly HAp\_a, is less translucent. This outcome is important as sample transparency enables direct viewing of living cells during biological characterization by light microscopy of the obtained materials. The achieved samples transparency can be directly associated with the related microstructures. Specifically, a product consisting of sub-micrometer sized hydroxyapatite grains was obtained after the consolidation of HAp\_b powders, while relatively coarser microstructures resulted in the HAp\_a and HAp\_c end-products. In addition, the transformation HAp to  $\beta$ -TCP occurred during sintering makes HAp\_a more sensitive to the chemical etching with respect to the other systems where the decomposition above was avoided.

The mechanical properties of the three HAp-based products are well comparable to those ones generally reported in the literature for apatites fabricated through alternative techniques. In particular, the higher hardness and elastic modulus are achieved for the HAp\_b system, whereas relatively lower values were obtained for the HAp\_a samples. Also these findings can be associated to thermal stability and microstructure of the starting powders. In particular, the significant amount of  $\beta$ -TCP formed during SPS when processing the HAp\_a powders is, along with the corresponding coarser microstructure, responsible for the resulting deterioration of the mechanical properties.

#### Acknowledgements

The financial support for this work from Regione Autonoma della Sardegna (Italy), L.R. n.7/2007, CUP n. F71J11001070002, is gratefully acknowledged. Two of us have performed their activity in the framework of the PhD in Biomedical Engineering (A.C.) and the International PhD in Innovation Sciences and Technologies (L.D.) at the University of Cagliari, Italy.

**References**

- Champion E., 2013, Sintering of calcium phosphate bioceramics, *Acta Biomater.*, 9, 5855-5875.
- Cihlar J., Buchal A., Trunec M., 1999, Kinetics of thermal decomposition of hydroxyapatite bioceramics, *J. Mater. Sci.*, 34, 6121–6131.
- Curran D.J., Fleming T.J., Towler M.R., Hampshire S., 2011, Mechanical parameters of strontium doped hydroxyapatite sintered using microwave and conventional methods, *J. Mech. Behav. Biomed. Mater.*, 4(8), 2063-2073.
- Dorozhkin S.V., 2010, Bioceramics of calcium orthophosphates, *Biomaterials*, 31, 1465-1485.
- Gilmore R.S., Katz J.L., 1982, Elastic properties of apatites, *J. Mater. Sci.* 17(4), 1131-1141.
- Hench L.L., Jones J.R., 2005, *Biomaterials, artificial organs and tissue engineering*. Woodhead Publishing Limited, Cambridge, UK
- Milman Yu.V., Golubenko A.A., Dub S.N., 2011, Indentation size effect in nanohardness, *Acta Mater.*, 59(20), 7480-7487.
- Musa C., Orrù R., Sciti D., Silvestroni L., Cao G., 2013, Synthesis, consolidation and characterization of monolithic and SiC whiskers reinforced HfB<sub>2</sub> ceramics, *J. Eur. Ceram. Soc.*, 33, 603-614.
- Nikzad L., Orrù R., Licheri R., Cao G., 2013, Influence of Mechanical and Electric Current Activation on the Mechanism of Formation and the Properties of Bulk B<sub>4</sub>C-TiB<sub>2</sub> Composites Obtained by Reactive Sintering, *Chemical Engineering Transactions*, 32, 1669-1674, DOI:10.3303/CET1332279
- Orrù R., Licheri R., Locci A.M., Cincotti A., Cao G., 2009, Consolidation/Synthesis of Materials by Electric Current Activated/Assisted Sintering, *Mater. Sci. Eng. R*, 63, 127-287.
- Oliver W.C., Pharr G.M., 1992, An Improved Technique for Determining Hardness and Elastic Modulus using Load and Displacement Sensing Indentation Experiments, *J. Mater. Res.*, 7(6). 1564-1583.
- Ramesh S., Aw K.L., Tolouei R., Amiryan M., Tan C.Y., Hamdi M., Purbolaksono J., Hassan M.A., Teng W.D., 2013, Sintering properties of hydroxyapatite powders prepared using different methods, *Ceram. Int.*, 39, 111-119.